Supplementary Information

"Bridging calorimetry and simulation through precise calculations of cucurbituril-guest binding enthalpies". Andrew T. Fenley, Niel M. Henriksen, Hari S. Muddana, and Michael K. Gilson.

Available Online Tutorial for Computing Binding Enthalpies

An online tutorial for direct enthalpy calculations, using the example of guest B2 binding to host CB7, will be posted with or shortly after publication of this article; see http://ambermd.org/tutorials/. The tutorial makes several adaptations, relative to the methods detailed here, for the sake of simplicity and computational speed. First, the number of explicit waters is set to exactly 1500 for each simulation. Second, for each simulation, a second NPT equilibration step is carried out at 1 bar, with the system's volume recorded every 100 fs. These volume data are used to calculate the average box volume associated with the pressure of 1 bar. The subsequent 500 ns production NVT run uses this average volume, and saves potential energy values every 1 ps. All other simulation parameters match the protocol used in main study. The resulting binding enthalpy is within k_bT of the value reported in the main text.

Alternative Decomposition of TIP3P Binding Enthalpies

In addition to the enthalpy decompositions provided in the main text, we also broke the computed binding enthalpies into contributions from changes in solute-solute (i.e., host-guest), solute-solvent, and solvent-solvent interactions. The results (Table S1) provide another indication of massive and systematic compensation among terms, particularly for the more highly charged guests, leaving relatively modest net changes in enthalpy.

Table S1. Binding enthalpies (kcal/mol) from experiment (expt), and calculations with the TIP3P water model (calc), along with decompositions of the calculated result into solute-solute, solute-solvent and solvent-solvent contributions, as noted.

Guest	ΔH(expt)	ΔH(calc)	ΔH(solute-solute)	ΔH(solute-solvent)	ΔH(solvent-solvent)
A1	-19.0 ± 0.2	-24.9 ± 0.2	-41.3	33.4	-17.0
A2	-19.3 ± 0.2	-22.7 ± 0.2	-111.4	163.2	-74.6
B2	-15.8 ± 0.1	-21.9 ± 0.2	-43.8	43.9	-22.0
B5	-15.6 ± 0.2	-18.3 ± 0.2	-172.9	286.2	-131.5
B11	-16.3 ± 0.2	-17.8 ± 0.2	-207.4	347.0	-157.4
G8	-8.5 ± 0.3	-6.2 ± 0.2	-138.3	241.3	-109.2
G9	-3.8 ± 0.1	-11.6 ± 0.2	-142.3	242.9	-112.1
MVN/Tris	-3.4 ± 0.2	-2.1 ± 0.2	-160.9	316.3	-157.6
MVN/NoTris	-3.4 ± 0.2	-4.7 ± 0.2	-154.8	277.5	-127.4

Results from TIP4P-Ew Water Model

This section presents further details of the binding enthalpy calculations obtained with the TIP4P-Ew water model, instead of TIP3P. As shown in Figure S1, these results correlate with experiment, but they yield a significantly larger offset (mean signed error -6.75 kcal/mol, y-intercept -6.4 kcal/mol) than the TIP3P results (mean signed error -2.97 kal/mol kcal/mol y-intercept -1.1 kcal/mol).

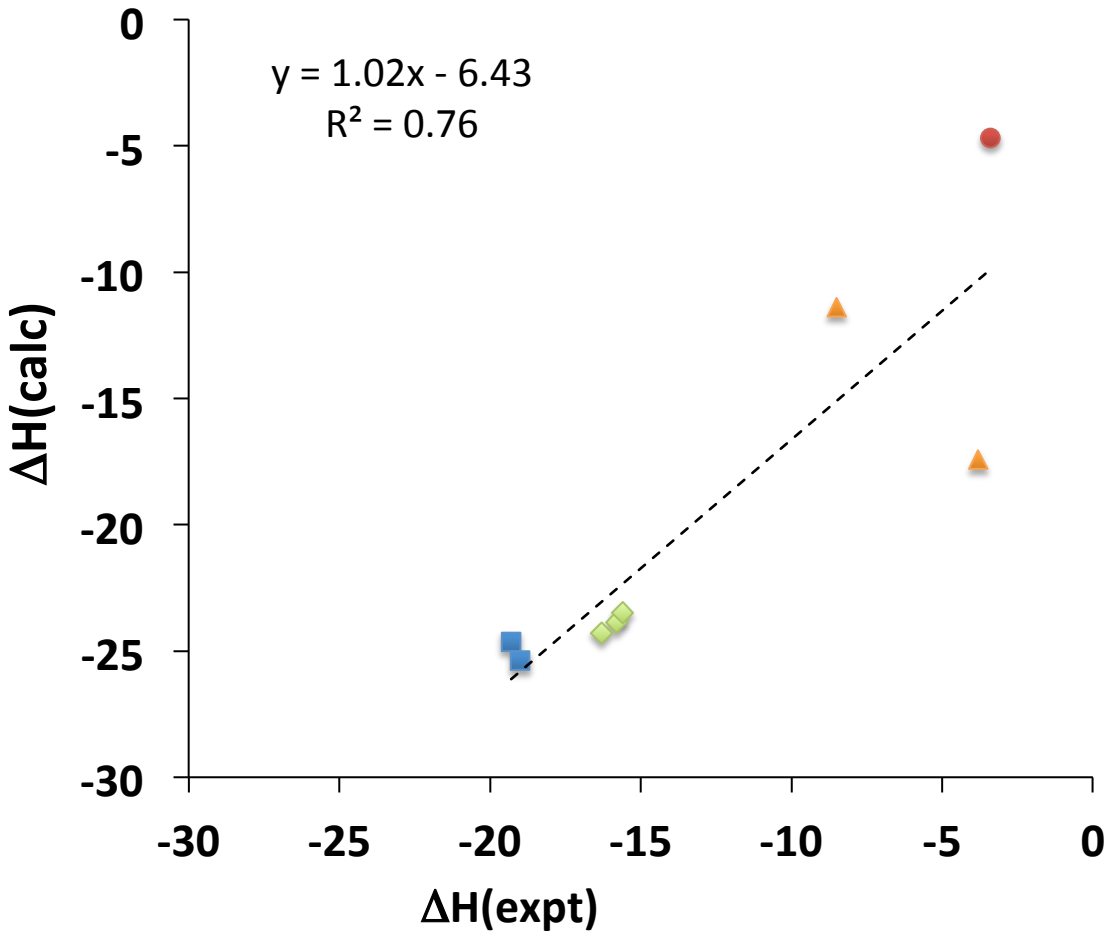

Figure S1. Comparison of binding enthalpies (kcal/mol) from experiment (expt) and simulation with TIP4P-EW water model (calc), for CB7 with eight guest molecules. Blue squares: adamantyl derivatives, A1, A2. Green diamonds: bicyclo[2.2.2]octane derivatives: B2, B5. Orange triangles: G8, G9. Red circle: MVN (Tris included in simulation).

The decomposition of the TIP4P-Ew binding enthalpies into energy terms, Table S2, may be compared with the corresponding decomposition for TIP3P, Table 2 in the main text. The Lennard-Jones contributions again are uniformly favorable, consistent with net increases in the number of atoms close to the host and guest in the bound versus the free states (ΔN_{close}). However, the net electrostatic contributions now are uniformly favorable. This increase in electrostatic interactions correlates with TIP4P-Ew's overestimation of the overall binding enthalpies, and may derive, at least in part, from the fact that TIP4P-Ew somewhat underestimates the dielectric constant of water[1]. However, more subtle factors may also be involved.

Table S2. Analysis of binding enthalpies (kcal/mol) computed with the TIP4P-Ew water model. Tot: total computed enthalpy change on binding. LJ: Lennard-Jones contribution. Elec: Coulombic electrostatic contribution. Val: contribution from changes in bond-stretch, angle-bend, and dihedral terms. Charge: net charge of the guest (e). N_{close}: change on binding in the number of atoms, either solute or solvent, within 4.25 Å of any atom of the host and guest.

	ΔH(calc)					
Guest	Tot	LJ	Elec	Val	Charge	ΔN_{close}
A1	-25.4	-12.2	-10.9	-2.4	0	239
A2	-24.6	-14.1	-8.6	-1.9	1	248
B2	-23.9	-9.2	-13.2	-1.4	0	206
B5	-23.5	-10.9	-12.3	-0.3	2	222
B11	-24.3	-13.4	-11.2	0.3	4	248
G8	-11.4	-11.0	-4.8	4.4	2	188
G9	-17.4	-9.5	-10.5	2.5	2	197
MVN/Tris	-4.7	6.0	-11.6	0.9	2	-241
MVN/noTris	-11.4	-2.6	-11.0	2.2	2	24

The TIP4P-Ew results are decomposed into solute-solute, solute-solvent, and solvent-solvent terms in Table S3, which is analogous to Table S1 for TIP3P, above.

Table S3. Binding enthalpies (kcal/mol) from experiment (expt), and calculations with the TIP4P-Ew water model (calc), along with decompositions of the calculated result into solute-solute, solute-solvent and solvent-solvent contributions, as noted.

Guest	ΔH(expt)	ΔH(calc)	ΔH(solute-solute)	ΔH(solute-solvent)	ΔH(solvent-solvent)
A1	-19.0 ± 0.2	-25.4 ± 0.2	-41.1	36.4	-20.7
A2	-19.3 ± 0.2	-24.6 ± 0.2	-110.5	162.7	-76.8
B2	-15.8 ± 0.1	-23.9 ± 0.2	-43.8	46.8	-26.9
B5	-15.6 ± 0.2	-23.5 ± 0.2	-171.7	283.6	-135.4
B11	-16.3 ± 0.2	-24.3 ± 0.3	-197.2	328.6	-155.6
G8	-8.5 ± 0.3	-11.4 ± 0.2	-136.3	239.7	-114.9
G9	-3.8 ± 0.1	-17.4 ± 0.2	-141.1	243.6	-119.9
MVN/Tris	-3.4 ± 0.2	-4.7 ± 0.2	-159.6	315.1	-160.1
MVN/NoTris	-3.4 ± 0.2	-11.4 ± 0.3	-151.4	272.7	-132.7

Simulation Convergence and Numerical Error Analysis

Blocking analysis[2] was used to estimate the standard deviation of the mean (σ) potential energy for each simulation. The reported standard deviations of the mean values are based on the use of 1000 blocks for each simulation which corresponds to 2 ns worth of frames per block. Most of the blocking analysis plots plateau by 200 ps worth of data per block (100 blocks), and all by the 2.0 ns time. We used blocks of 2.0 ns to evaluate the standard deviations of the mean values. Extending the block sizes from 200 ps to 2.0 ns led to increases in the estimated standard deviation of the mean of at most 0.005 / 0.012 kcal/mol (TIP3P / TIP4P-Ew). Furthermore, we note that the estimates of the standard deviation of the mean from blocking analysis were independently verified via direct calculation of the autocorrelation function. The associated statistical inefficiency values[3] point to autocorrelation times of the potential energy estimates that are less than 1.0 ps. Table S4 details the resulting standard deviation value for all simulations, along with the resulting uncertainties in the binding enthalpies for all guests.

Table S4. Standard deviation of the mean (σ) potential energy (kcal/mol) for all simulations, both without (Free) and with (Host) present for both water models (TIP3P / TIP4P-Ew). The estimated numerical error of the binding enthalpy is computed by adding the σ values of the individual simulations in quadrature. The Solvent - σ Free values are for solvent without either host or guest, and the Solvent - σ Host values are for solvent with host but no guest. All other rows are for simulations including the indicated guest, without and with the host.

TIP3P / TIP4PEW	σ Free	σ Host	Total Binding Enthalpy Error
Solvent/Tris	0.10 / 0.12	0.10 / 0.12	
Solvent/NoTris	0.06 / 0.12	0.07 / 0.12	

A1	0.10 / 0.12	0.11 / 0.12	0.2 / 0.2
A2	0.07 / 0.12	0.11 / 0.13	0.2 / 0.2
B2	0.10 / 0.12	0.10 / 0.12	0.2 / 0.2
B5	0.10 / 0.12	0.10 / 0.12	0.2 / 0.2
B11	0.11 / 0.13	0.11 / 0.13	0.2 / 0.3
G8	0.10 / 0.12	0.11 / 0.13	0.2 / 0.2
G9	0.10 / 0.12	0.10 / 0.12	0.2 / 0.2
MVN/Tris	0.10 / 0.12	0.10 / 0.13	0.2 / 0.2
MVN/NoTris	0.10 / 0.13	0.10 / 0.13	0.2 / 0.3

We also investigated whether or not estimates of the standard deviation of the mean for the nonbonded force field terms (e.g. Lennard-Jones and electrostatics) differ significantly from the standard deviation of the mean for the total potential energy. The standard deviation of the mean for the nonbonded components to the enthalpy change on binding is 0.27 kcal/mol for the guests G8 and G9 binding to CB7. This is somewhat larger than the standard deviation of the mean for the total binding enthalpy for the same guests, 0.17 kcal/mol, so there must be anticorrelation among the fluctuations of individual energy components. Nonetheless, 0.27 kcal/mol remains small relative to the physically interesting differences of the nonbonded components across the different host-guest systems.

The valence component of the binding enthalpy is particularly unfavorable (at least 2.5 kcal/mol) for both G8 and G9. Direct computation of the standard deviation of the mean of the valence term yields a value of 0.01 kcal/mol for each independent simulation. The combined standard deviation of the mean of the valence component for the full binding cycle is 0.02 kcal/mol. Therefore, the striking valence penalty upon binding for G8 (over 4 kcal/mol) and G9 (over 2.5 kcal/mol) is statistically significant.

Figure S2 shows the convergence graphs and blocking analyses for all four simulations used to compute the binding enthalpy of CB7 with B11, the most flexible and highly charged (+4) guest. Orientational sampling of this guest around the symmetry axis of CB7 is demonstrated in Figure S3, which shows a representative snapshot of the complex, along with a time-averaged structure where all snapshots were aligned based on the host. Thorough orientational sampling is confirmed by the fact that the averaged guest coordinates fall on the host's symmetry axis.

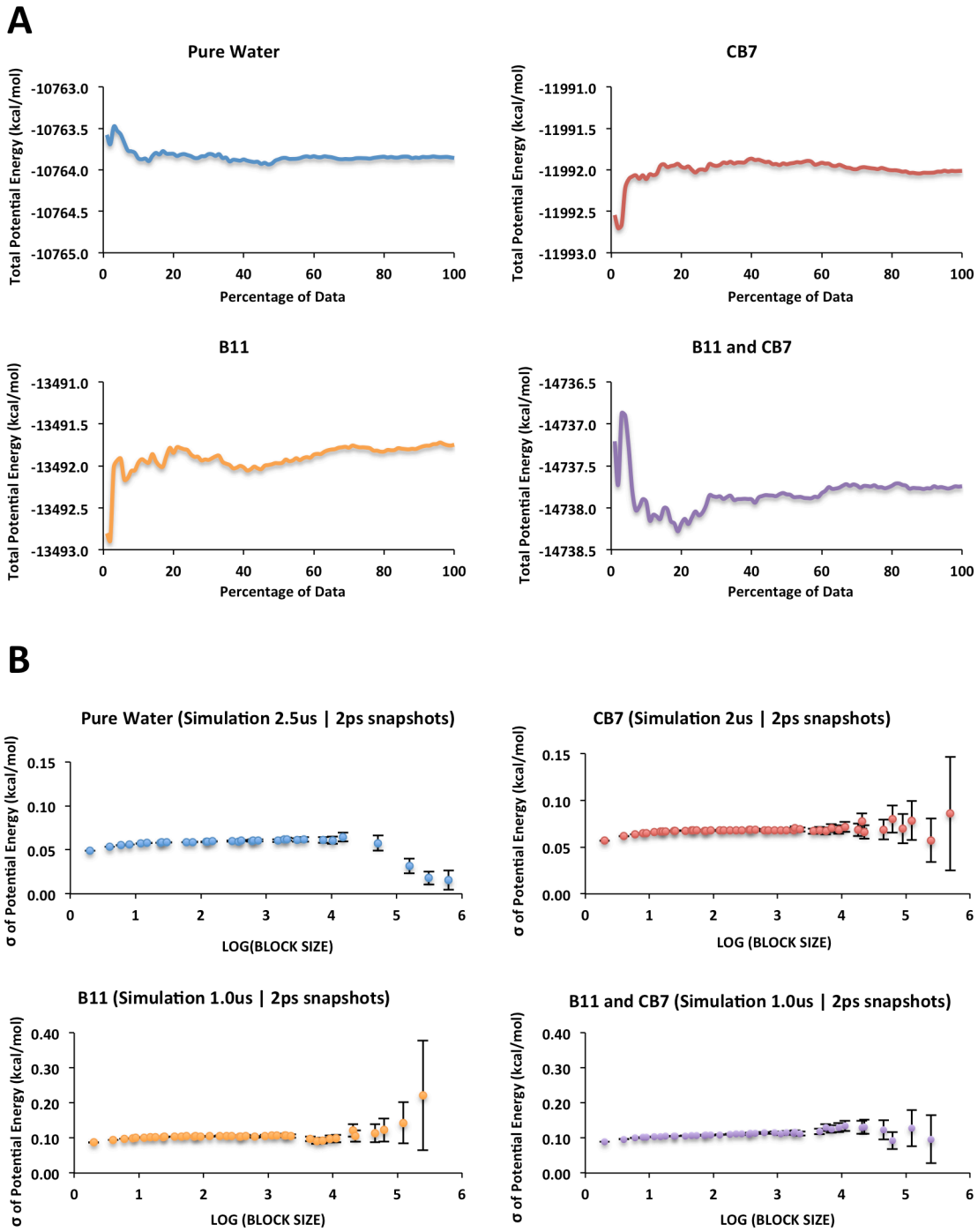

Figure S2. Convergence and blocking analysis of the four simulations with TIP3P water used to compute the binding enthalpy of guest B11 with CB7. **A** Convergence of the total potential energy for each simulation as a function of total simulation data. **B** Blocking analysis for each simulation.

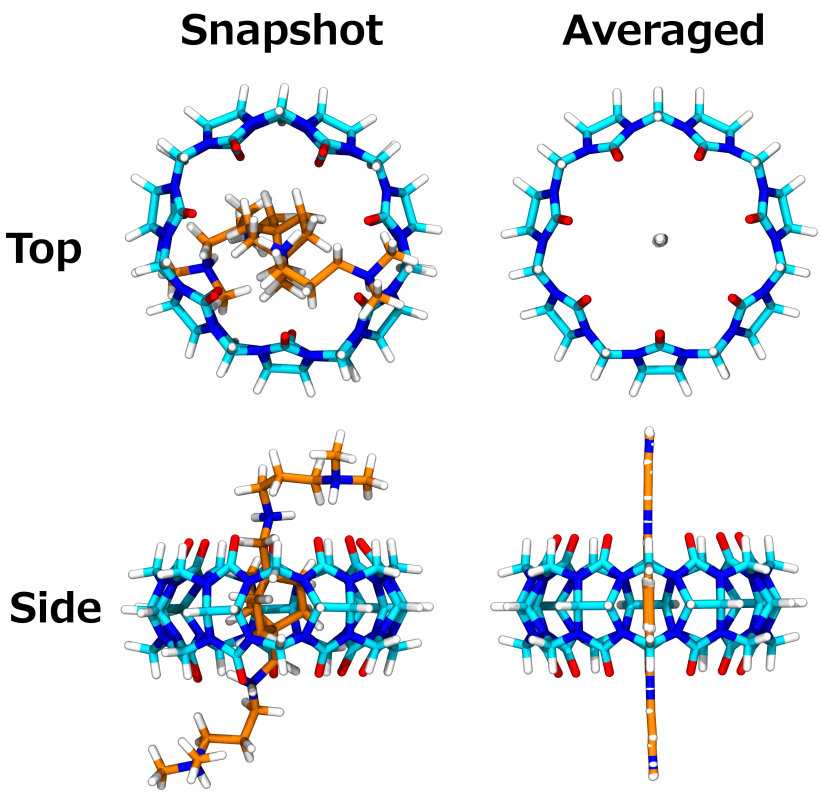

Figure S3. Graphical representation of thorough conformational sampling for the complex of CB7 with the most flexible guest, B11. Left: a single conformational snapshot, from two viewpoints. Right: conformation obtained as an average of Cartesian coordinates over the entire 1 μs simulation, where snapshots were aligned based on the coordinates of CB7. Water molecules, present in the simulation, are omitted from this figure.

Sensitivity to Simulation Parameters and Approximations

NPT versus NVT simulations

Production simulations are often carried out under conditions of constant volume, for the sake of computational performance, with the volume locked at that of the last snapshot of a constant pressure equilibration simulation. However, the normal fluctuations of the volume during the constant pressure equilibration stage mean that the volume used in the subsequent production run may be significantly different from the mean volume associated with the intended pressure. We therefore ran additional binding enthalpy calculations for CB7 with guest A2, in order to examine the sensitivity of the mean potential energy to the choice of volume. Thus, for each system (CB7-A2 complex, pure water, free A2 and free CB7), we ran three NVT simulations, each for an additional 100 ns after the 1 μs NPT production run, where the box volumes were set to: a) the average box volume from the previous 1 μs; b) the smallest box volume generated during the 1 μs NPT run; and c) the largest box volume generated during the 1 μs NPT run. As shown in Figure S4 and Table S5, the mean energies and resulting binding enthalpy vary significantly with box volume. As expected, the binding enthalpy estimate from NVT simulations using the average volumes from the corresponding prior NPT runs closely matches the reference NPT result to

within 0.3 kcal/mol. However, the binding enthalpy estimate from the largest volume simulations deviates by 1.8 kcal/mol, and the binding enthalpy estimate from smallest volume simulations deviates -9.5 kcal/mol. The pathology is exacerbated if one combines potential energy estimates from simulations whose volumes deviate above and below their NPT averages, which is a realistic possibility with common simulation practices. The worst-case scenario for the present set of simulations occurs when one combines the large volume simulations for the pure water and complex with the small volume simulations for the free guest and free host: the result is a computed binding enthalpy 161 kcal/mol less favorable than the estimate from the NPT simulations. Based on this analysis, we opted to compute binding enthalpies with average energies obtained from NPT production runs.

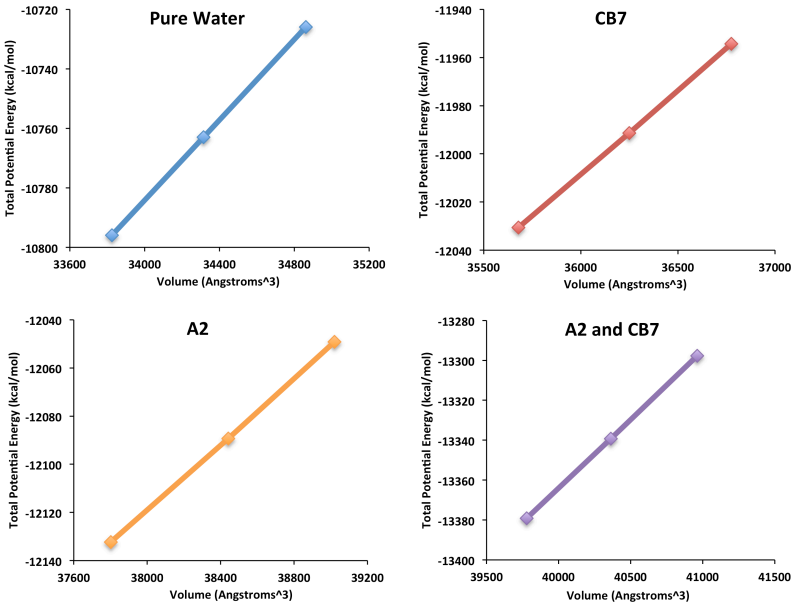

Figure S4. Graphs of mean energies versus volume for the four simulations used to calculate the binding enthalpy of A2 with CB7.

Table S5. Average potential energies and binding enthalpies (kcal/mol) computed for the host-guest pair CB7-A2 with TIP3P explicit water in the NVT ensemble at various volumes, with the NPT result provided for reference.

	CB7-A2	Water	A2	CB7	ΔH	ΔΔH
NPT (Reference)	-13340.13	-10763.84	-12090.15	-11991.99	-21.8	0.0
NVT-Average Volumes	-13339.31	-10762.94	-12089.29	-11991.39	-21.6	0.3
NVT-Largest Volumes	-13297.69	-10725.94	-12049.23	-11954.36	-20.1	1.8
NVT-Smallest Volumes	-13379.20	-10795.96	-12132.26	-12030.61	-12.3	9.5
NVT-Worst Case	-13297.69	-10725.94	-12132.26	-12030.61	139.2	161.0

Single-, Double, and Mixed Precision Simulations

In order to improve computational performance, AMBER's GPU code currently defaults to a mixture of single precision and fixed point (SPFP) variables for computing and storing values throughout the simulation[4]. We investigated how the precision of the integrator affects the present calculations for CB7 and A2, by taking advantage of the fact that the code can be recompiled to carry out all GPU calculations and accumulation of stored values in double precision (DPDP). We extended the current 1 μs simulations of free CB7, pure water, free A2, and the complex CB7-A2 each for an additional 200 ns, using both the SPFP and DPDP compiled integrators. Care was taken to ensure that, while the random number seed for assigning velocities was different among the four simulations, the same seed value was assigned for the SPFP and DPDP versions of each simulation. Therefore any drift in the measured energies resulted only from the difference in integrators. As shown in Table S6, switching from SPFP to DPDP changed the mean potential energies by no more than 0.13 kcal/mol, which is commensurate with the standard deviation of the mean. Thus, the use of the SPFP mixed precision model does not appear to have an adverse effect on the binding enthalpy calculations.

Table S6. Average potential energies and binding enthalpies (kcal/mol) for the host-guest pair CB7-A2 with TIP3P explicit water, from 200 ns simulations in the NPT ensemble, using either the SPFP or DPDP integrator.

	CB7-A2	**WATER**	**A2**	**CB7**	**ΔH**
SPFP (200 ns)	-13340.87	-10764.04	-12089.93	-11992.06	-22.92
DPDP (200 ns)	-13340.92	-10763.99	-12089.97	-11991.93	-23.01
Difference	-0.05	0.05	-0.04	0.13	-0.09

Nonbonded Cutoff Distance

We examined the sensitivity of the binding enthalpy computed for CB7 and A2 to the choice of the Lennard-Jones interaction cutoff, by recomputing the potential energy for every snapshot in the four DPDP simulations mentioned above, using a distance cutoff of 14 Å (the maximum value for the box size when generating the nonbonded pair list) instead of 9 Å. As shown in Table S7, the differences in the individual mean energies are within 0.17 kcal/mol, and the change in the resulting binding enthalpy is 0.07 kcal/mol, which is within the numerical uncertainty. Therefore, the 9 Å cutoff distance appears to be adequate.

Table S7. Average potential energies and binding enthalpy (kcal/mol) for CB7 and A2, with TIP3P explicit water, from 200 ns simulations in the NPT ensemble using the original cutoff (9 Å) or a longer cutoff (14 Å).

	CB7-A2	**WATER**	**A2**	**CB7**	**ΔH**
9 Å Cutoff	-13340.92	-10763.99	-12089.97	-11991.93	-23.01
14 Å Cutoff	-13341.10	-10763.91	-12090.00	-11992.06	-22.94

Difference	0.17	-0.08	0.03	0.14	-0.07

Long range Lennard-Jones corrections[5,6] were also applied during the simulations used in this study. While these correction values are constant for a given system's atomic composition, box volume, and cutoff value, and thus do not contribute to the forces during the simulation, their values can be significant in magnitude and are always favorable. However, we found that the net impact of these corrections on the binding enthalpy estimate is negligible. As shown in Table S8, the difference in binding enthalpy of B2 with CB7 with the corrections turned on or off is only -0.09 kcal/mol. This difference is well within the standard deviation of the mean of the binding enthalpy estimate.

Table S8. Average potential energies and binding enthalpies (kcal/mol) for CB7 and B2, with TIP3P explicit water, with long range LJ corrections turned on or off. Both calculations used the same set of snapshots, which were generated by a simulation that with the long-ranged LJ correction turned on.

	CB7-B2	**WATER**	**B2**	**CB7**	**ΔH**
LJ Correction On	-12567.16	-10763.86	-11317.05	-11992.01	-21.95
LJ Correction Off	-12487.95	-10700.49	-11248.96	-11917.63	-21.85
Difference	-79.20	-63.37	-68.10	-74.38	-0.09

Number of water molecules

Some of the present simulations have $N_{w,AB+} \neq N_{w,B+}$ due to a slight imbalance in the number of waters (33 for TIP3P and 31 for TIP4P-Ew) between the simulations. To check for any possible consequences due to the small difference in chloride concentration, we reran the B11 and pure water simulations for the TIP3P water model, with the water counts exactly matched between the B11 free and bound simulations. We chose B11 because this is the guest with the greatest charge (+4), and hence the most chloride counterions and, presumably, the maximal consequences of counterion dilution. The simulation with matched water counts agreed with the prior simulation to within -0.04 kcal/mol. We also tested whether or not adding an additional ~1000 waters to the bound and unbound simulation of cationic guest B5, for both water models, would change the results. For TIP3P, the enthalpy estimate was shifted by 0.24 kcal/mol, and for TIP4P-Ew, the estimate was shifted by 0.26 kcal/mol. Especially given the increased energy fluctuations for these larger water boxes, this shift is commensurate with the estimated uncertainties of the mean potential energies. Thus, the concentration of chloride counterions does not appear to be a significant determinant of the computed binding enthalpies.

Ion Balance in Binding Enthalpy Calculations

We consider the case of a cationic guest, B+, which binds a neutral host, A, to form the cationic complex AB+. The definition of the binding enthalpy as the difference in the partial molar enthalpies of the products versus the reactants is:

$$\Delta H = h_{AB+} - h_A - h_{B+}$$

Following the formalism in the manuscript, the partial molar enthalpies are written as differences in mean energy, now explicitly considering that the energy calculations for the cationic species include a dissolved Cl- anion necessary to set the total charge 0 within the simulations:

$$h_{AB+} = U_{AB+,N_{w,AB+},Cl-} - U_{N_{w,AB+},Cl-}$$

$$h_A = U_{A,\mathrm{N}_{w,A}} - U_{N_{w,A}}$$

$$h_{B+} = U_{B+,\mathrm{N}_{w,B+},Cl-} - U_{N_{w,B+},Cl-}$$

The notation here matches the manuscript such that, $U_{AB+,N_{w,AB+},Cl-}$ is the mean energy for the cationic host-guest complex with $N_{w,AB+}$ water molecules and one chloride ion. Thus,

$$\Delta H = \left(U_{AB+,\mathrm{N}_{w,AB+},Cl-} - U_{A,\mathrm{N}_{w,A}} - U_{B+,\mathrm{N}_{w,B+},Cl-}\right) - \left(U_{N_{w,AB+},Cl-} - U_{N_{w,A}} - U_{N_{w,B+},Cl-}\right)$$

If the simulations are set up such that $N_{w,AB+} = N_{w,B+}$, then the mean potential energies of the chloride ion in pure water will cancel between the bound and unbound states:

$$U_{N_{w,AB+},Cl-} = U_{N_{w,B+},Cl-}$$

so that we are left with,

$$\Delta H = \left(U_{AB+,\mathrm{N}_{w,AB},Cl-} - U_{A,\mathrm{N}_{w,A}} - U_{B+,\mathrm{N}_{w,B},Cl-}\right) + U_{N_{w,A}}$$

as the total enthalpy of binding.

Details of Energy Minimization and Equilibration Procedure

Prior to production simulations, each system underwent multiple stages of energy minimization, followed by equilibration with a Langevin thermostat[7] and Berendsen barostat[8]. Energy minimization proceeded in five steps, where the first four steps involved a gradual reduction of harmonic restraints applied to the solute(s). The harmonic restraints were 500.0, 100.0, 20.0, and 1.0 kcal/mol/Å^2 in strength, to allow only the water to relax via, respectively, 500, 500, 250, and 100 steps of steepest descent followed by up to 4,000 steps of conjugate gradient minimization until the root-mean-square of the gradient was less than 0.0001 kcal/mol-Å. The system was then further energy-minimized with the restraints removed for another 500 steps of steepest descent, again followed by up to 4,000 steps of conjugate gradient with the same convergence criterion as before. Equilibration of the system began by heating the system to 300K over 2 ns, using a Langevin thermostat with the collision frequency set to 1.0 ps^{-1}, in the NVT ensemble, with 2 fs integration steps, with the solute atoms restrained with 5.0 kcal/mol/Å^2 harmonic restraints. To finish the equilibration process, the restraints were removed, and the system was simulated in the NPT ensemble for 4 ns with a 1 fs integration time step, using the previous thermostat parameters and the Berendsen barostat with the pressure set to 1 bar and the relaxation time set to 2 ps. We validated the pressure regulation by running 500 ns of simulation for B2 bound to CB7, saving pressure data every 100 fs instead of every 2ps in order to gather more extensive statistics. This calculation yielded a mean pressure of 1 bar with a standard error of the mean equal to 0.12 bar and a standard deviation of the instantaneous pressure of 220 bar. Particle Mesh Ewald[9–11] was used to calculate the full electrostatic interaction energies in the periodic system for both the NVT and NPT simulations, and SHAKE[12] was turned on for all bonds involving hydrogen. Nonbonded interactions had a cutoff value set to 10.0 Å for all of the minimization and equilibration steps.

References

(1) Horn, H. W.; Swope, W. C.; Pitera, J. W.; Madura, J. D.; Dick, T. J.; Hura, G. L.; Head-Gordon, T. Development of an Improved Four-Site Water Model for Biomolecular Simulations: TIP4P-Ew. *J. Chem. Phys.* **2004**, *120*, 9665.

(2) Flyvbjerg, H.; Petersen, H. G. Error Estimates on Averages of Correlated Data. *J. Chem. Phys.* **1989**, *91*, 461–466.

(3) Chodera, J. D.; Swope, W. C.; Pitera, J. W.; Seok, C.; Dill, K. A. Use of the Weighted Histogram Analysis Method for the Analysis of Simulated and Parallel Tempering Simulations. *J. Chem. Theory Comput.* **2006**, *3*, 26–41.

(4) Le Grand, S.; Götz, A. W.; Walker, R. C. SPFP: Speed without compromise—A Mixed Precision Model for GPU Accelerated Molecular Dynamics Simulations. *Comput. Phys. Commun.* **2013**, *184*, 374–380.

(5) Allen, M. P.; Tildesley, D. J. *Computer Simulation of Liquids*; 1st ed.; Clarendon, Oxford, 1987.

(6) Shirts, M. R.; Mobley, D. L.; Chodera, J. D.; Pande, V. S. Accurate and Efficient Corrections for Missing Dispersion Interactions in Molecular Simulations. *J. Phys. Chem. B* **2007**, *111*, 13052–13063.
(7) Pastor, R. W.; Brooks, B. R.; Szabo, A. An Analysis of the Accuracy of Langevin and Molecular Dynamics Algorithms. *Mol. Phys.* **1988**, *65*, 1409–1419.
(8) Berendsen, H. J. C.; Postma, J. P. M.; van Gunsteren, W. F.; DiNola, A.; Haak, J. R. Molecular Dynamics with Coupling to an External Bath. *J. Chem. Phys.* **1984**, *81*, 3684–3690.
(9) Darden, T.; York, D.; Pedersen, L. Particle Mesh Ewald: An N · log(N) Method for Ewald Sums in Large Systems. *J. Chem. Phys.* **1993**, *98*, 10089–10092.
(10) Essmann, U.; Perera, L.; Berkowitz, M. L.; Darden, T.; Lee, H.; Pedersen, L. G. A Smooth Particle Mesh Ewald Method. *J. Chem. Phys.* **1995**, *103*, 8577–8593.
(11) Crowley, M.; Darden, T.; Iii, T. C.; Ii, D. D. Adventures in Improving the Scaling and Accuracy of a Parallel Molecular Dynamics Program. *J. Supercomput.* **1997**, *11*, 255–278.
(12) Ryckaert, J.-P.; Ciccotti, G.; Berendsen, H. J. . Numerical Integration of the Cartesian Equations of Motion of a System with Constraints: Molecular Dynamics of N-Alkanes. *J. Comput. Phys.* **1977**, *23*, 327–341.